Hydrothermally engineered enhanced hydrate formation for potential CO_2 capture applications

Mohd Hafiz Abu Hassan[1], Farooq Sher[2,*], Saba Sehar[3,4], Tahir Rasheed[5], Ayesha Zafar[4,6], Jasmina Sulejmanović[7], Usman Ali[8], Tazien Rashid[9]

[1]*Fakulti Sains dan Teknologi, Universiti Sains Islam Malaysia, 71800 Nilai, Malaysia*

[2]*Department of Engineering, School of Science and Technology, Nottingham Trent University, Nottingham NG11 8NS, United Kingdom*

[3]*Department of Chemistry, University of Agriculture, Faisalabad 38040, Pakistan*

[4]*International Society of Engineering Science and Technology, Nottingham, United Kingdom*

[5]*School of Chemistry and Chemical Engineering, Shanghai Jiao Tong University, Shanghai, 200240, China*

[6]*Institute of Biochemistry and Biotechnology, Faculty of Biosciences, University of Veterinary and Animal Sciences, Lahore 54000, Pakistan*

[7]*Department of Chemistry, Faculty of Science, University of Sarajevo, 71 000, Sarajevo, Bosnia and Herzegovina*

[8]*Department of Chemical Engineering, University of Engineering and Technology, Lahore 54890, Pakistan*

[9]*Department of Chemical Engineering, NFC Institute of Engineering and Fertilizer Research, Faisalabad, Pakistan*

*Corresponding author:
Dr. F. Sher
Assistant Professor
Department of Engineering, School of Science and Technology
Nottingham Trent University
Nottingham
NG11 8NS
UK
E-mail address: Farooq.Sher@ntu.ac.uk
Tel.: +44 (0) 115 84 86679

Abstract

Gas hydrate formation is regarded as the emerging technology to mitigate the effect of greenhouse gases. Now a day, the alarming situation of increased CO_2 concentration of about 450 ppm is associated with elevation of earth temperature up to 2 °C. Where the CO_2 hydrate ($CO_2.6H_2O$) formation is of environmental and scientific interest due to carbon capture and storage (CCS) in order to condense environmental CO_2 concentration. The present study is experimentally addressing the four different sample preparation procedures (method 1, 2, 3 and 4) of stirring for the CO_2 hydrate ($CO_2.6H_2O$) formation correlated with the integrated gasification combine cycle (IGCC) conditions. A high-pressure volumetric analyzer (HPVA) is used to explore the rate of CO_2 hydrate formation that is critically investigated using pressure-time (P-t) curves for all the prepared samples. The highest stirring (method 4) speed with 37000 rpm, had the highest moisture content of 14.8 wt% as well as at 275 K and 36 bar. By using method 4 hydrate conversion of 40.5 mol% was observed. The high stirring method (method 4) show gas uptake of about 3.9 mmol of carbon dioxide per gram of H_2O and the highest rate for formation of hydrate as 0.05 mmol of carbon dioxide per gram of H_2O per min. Further, comparison of promoter's combination relative to long experiment duration resulted in the increment of 13.82 mol% of water to hydrate conversion in 2600 min at 283 K and 58 bar for T1-5 (having 5.6 mol% of THF and 0.01 mol% of SDS) as compared to the experiment that was performed in 1200 minutes.

Keywords: Environment; CO_2 utilisation; Pollution; Greenhouse effect; Gas hydrate; Emissions, Carbon capture and storage (CCS).

1. Introduction

The energy sector, especially industrialization uses a major part of the earth energy and in return produces hazardous greenhouse gases as a societal alarm. The burning of fossil fuels (natural gas, coal and oil) in power machines for industrial manufacturing and transportations

have increases the CO_2 contents in the air, thus act as a major source of global warming. Human activities increase the CO_2 concentration around 280–404 ppm during the era of 1750–2016, which is about 45% greater than pre-industrial revolutions level. The globe means sea level reflects 20 cm increase with the 1 °C elevation in average global temperature during 1901–2010 [1, 2]. About 80% reduction in greenhouse gases is included in the strategies of the European Union till 2050. Carbon capture and sequestration (CCS) is known as decarbonisation technology and will be available in electricity cost up to 2030 successfully for the reduction of environmental threats.

CCS is a step-wise process of CO_2 capturing from industries, power plants and natural gas wells (having high CO_2 levels) for mitigation of global warming [3]. The estimated temperature reduction below 2 °C can be handle easily with the implementation of CCS [4]. Some conventional strategies are also used for the consumption of CO_2 such as polymer-based nanocomposite, physio-chemical absorbents, cryogenic systems, membranes, chemical looping combustion via metal oxides and hydrate based gas separation (HBGS) [5-8]. CO_2 can be stored via pipelines to un-mineable coal layers, saline aquifers, underground geological storage, sea beds mineral carbonation, depleted oil/gas fields and gas hydrate storage capture [1]. Among these, underground mineral storage has the disadvantage of leakage through an earthquake. The estimated temperature reduction below 2 °C can be handle easily with the implementation of CCS. Thus, CCS technology can be applied for the pre-combustion and post-combustion collection of carbon dioxide.

The pre-combustion capture is commonly used to consume CO_2 from fuel gas mixtures [9]. This pre-consumption of CO_2 is successfully used as in an IGCC (integrated gasification combined cycle), which is the most important technique used for the reduction of the rate of

CO_2 emission from chemical power plants. This technology is implemented to convert fossil fuels into fuel gas (60% CO_2 and 40% H_2) mixture and precise pressure range in the outlet stream of about 2–7 MPa [10]. Certain CO_2 gas separation challenges are also associated with IGCC, making it a 75–80% high-cost method. So, should be modified to get cheap CO_2 removal conditions of pressure and temperature [5]. Among all the above-mentioned methods, HBGS is extensively used on behalf of its low cost as compared to the IGCC power plant [11].

Gas hydrate is a type of crystalline solid that has trapped gas (guest) molecules in the water (host) cage. The solubility of hydrate formers in water and contact area of hydrate former with water is a very important factor in hydrate formation [12]. These reduce the mass transfer problems and thus facilitate the hydrate formation process. Besides the fact of more suitability of the HBGS process for pre-combustion CO_2 capture from fuel gas mixture as well as applicability in post-combustion capture of CO_2 from flue gas [13]. The reason can be best explained based on 1000 times high fuel gas pressure (40% CO_2 and 60% H_2) as compared to flue gas (17% CO_2 and 83% N_2) [14] and about 99 mol% CO_2 can be recovered from the fuel gas [9]. The HBGS process requires gas molecules (O_2, H_2, N_2 and CO_2), high pressure (10-70 bar) gas component and 273 K temperature for the formation of non-stoichiometric compounds. Hydrate formation has potential application with flow assurance in the oil and gas industry. On the other hand, it also has paramount utilization in refrigerators, air conditioners and gas storage applications [15].

It has been studied that the CO_2 capturing is Cross-Linked Enzyme Aggregates (CLEAs) to bovine carbonic anhydrase (BCA) with the assistance of magnetic field technique and magnetic nanoparticles with a maximum immobilization yield of 84% [16]. Park et al., [17]

mixed an amount of water identical to the pore volume of silica gel inside the bottle consisting of dry silica gel and an ultrasonic wave was used to blend them. Another study explains the effect of impeller efficiency on the CO_2 based formation of hydrate and finds out the 4 times more rate of hydrate formation with six blades as compared to three blades for stirring with reduced equilibrium time up to half [18]. In another work, hydrophobic silica was mixed with an alkaline solution and then the mixture was stirred at 37000 rpm for 30 seconds to prepare a porous sample for CO_2 capture investigation at low pressure (2–3 bar) [19].

Thus, this study investigates the advantage of continuous stirring to prepare the sample and its effect on the formation of hydrate inside a fixed bed reactor (FBR) or HPVA. Silica gel was used as a solid adsorbent (porous medium) which omit the need of stirring process inside the reactor during hydrate formation. Pre-combustion capture has been chosen in this study rather than post-combustion and oxyfuel combustion due to its high shifted gas pressure where the partial pressure of CO_2 is in the range of 8–28 bar. It can separate H_2 gas from fuel gas which can produce future clean energy [20]. Therefore, this study will help in providing a suitable sample preparation method for the formation of hydrate inside any reactor that employs adsorbent as a porous medium. Parameters such as promoters, rate of stirring and water contents have been studied by using solid adsorbent. To the best of our knowledge, for the first time, this research reports the best determination method to prepare solid adsorbent as a medium for CO_2 hydrate formation. Consequently, four sample preparation methods by using solid adsorbents in the gas capture field were studied.

2. Experimental

2.1. Materials

The mesoporous silica gel as adsorbent having 5.14 nm pore size, 200–500 µm particle size, pore volume of 0.64 cm^3/g with a surface area of 499 m^2/g and CO_2 obtained from Fisher

Scientific. Helium (He) (99.99% purity) at 34.4 bar partial pressure used for venting or cleaning purposes. The compressed air or nitrogen (N_2) with 5.2–5.5 bar was used for controlling the pneumatic valves. These were purchased from BOC (Brin's oxygen company). An anti-freezing agent was purchased from ASDA (Asquith and dairies). All the materials were used without further purifications.

2.2. Sample preparation methods

During the preparation of wet silica gel, four methods were used, namely method 1 (silica was left to naturally adsorbed moisture), method 2 (the lowest rates of stirring of silica), method 3 (silica was submerged in excess water) and method 4 (the highest rates of stirring of silica). For all methods, dried the silica gel in the oven (Model AX30 and Carbolite manufactured with 40–250 °C temperature limits) at 200 °C for one night before the experiment. Finally, each final equilibrium mass of wet silica gel was deducted with this dry silica gel mass to obtain the final moisture content respectively.

During method 1, 2.5 g dried silica gel (by weighing the balance of AE Adam manufacturers having Model AEA-220 A in the range of 0.01–220 g) was placed inside a weighing boat and left at atmospheric condition to attained equilibrium. During the sample preparation method 2, placed the 2.5 g of dry silica gel and 50 times excess of water in a beaker. After absorbing water, the total mass became 50 g. Then, silica gel was slowly stirred in water by using a magnetic stirrer overnight. Finally, the beaker was placed at atmospheric condition until the mass of the whole mixture attained equilibrium.

During method 3, take 0.5 g dry silica gel that is placed in a weighing boat with an excess of water. So that the whole mixture attained a mass of about 50 g. Then, repeat the same process for attaining the equilibrium. On the other hand, method 4 used 0.5 g dry silica gel, which is

placed in a weighing boat with an excess of water. Therefore, that the whole mixture mass reached up to 50 g. Further, high-speed blender at 3700 rpm vigorously stirred the silica gel sample in the presence of water for 90 sec. [19]. Method 4 can be recognized as the high stirring method due to its high speed of stirring as compared to methods 1, 2 and 3. Finally placed the whole stirred mixture in open atmospheric conditions to attain equilibrium.

Three promoters (supplied by Fisher Scientific) were used (separately or in combined form) such as-THF and SDS with almost 99% purity. All the promoters dissolved in water for the sake of dilution to obtain the relevant concentration of promoters by using a continuous stirring method (method 4). Each sample was prepared with 2.5 g of dry silica gel with a promotor-water solution of 47.5 g. The specific concentration used for each single or combined promoter, silica gel and water employed in this work is presented in **Table 1**. Thus, the overall mixture attains a mass of 50 g [21, 22]. On the other hand, T1-5 was prepared by mixing the 5.6 mol% of THF with 0.01 mol% of SDS by employing the same type of silica gel as an adsorbent. As for zeolite (13X) and X13-5 type of promoter were obtained from Sigma-Aldrich was combined with THF and SDS.

2.3. Working principles of HPVA

The HPVA-100 as shown in

Fig. 1 is provided by Micromeritics. It was used to attain isotherm related to high pressure with the use of volumetric method. Firstly, the silica gel was loaded in the sample cell and placed in the furnace. It was carefully noted that the valve (V1) of the cell was closed. Then, the furnace was heated to 200 °C by temperature controller and at the same time, the vacuum pump (V3) was switched on to vent out any gas and moisture present in the system through V2. When the operating temperature was obtained, then the valves were slowly unlocked up

to the maximum opening of V1. The experiment was left running overnight. Finally, calculate the equilibrium moisture content by using **Eq. (1)**.

$$Equilibrium\ moisture\ content\ (wt\%) = \frac{moisture\ content\ (g)}{wet\ silica\ gel\ (g)} \times 100\% \qquad (1)$$

The HPVA-100 can achieve a pressure of 100 bar and was used with a static volumetric method to attain high-pressure adsorption isotherms successfully. It includes the introduction of a specific amount of carbon dioxide (CO_2) as an adsorptive gas into the sample containing compartment [5]. Where the sample attained equilibrium in the presence of adsorbent with the repetition of the experiment at given pressure intervals. The process is repeated until the maximum fixed pressure interval is reached. The amount of adsorbed gas can be calculated by equilibrium pressure and volume as given in **Eq. (2)**.

$$(\Delta n_{\downarrow})_t = V_S \left(\frac{P}{zRT}\right)_0 - V_S \left(\frac{P}{zRT}\right)_t \qquad (2)$$

where z is the compressibility factor, V_S is the volume of the sample cell, R is the gas constant, P and T are the pressure and temperature of the sample cell [9]. In the sample chamber, transducers are used for sampling to obtained high accuracy and reproducibility. At first cell's valves remain closed before the introduction of CO_2 and the pre-experiment preparations include the three times purging of He gas to remove the impurities. The pre-defined operating conditions; gas port analysis, operating temperature and pressure and experiment time are applied. Further antifreeze agent having 70% water + 30 vol% was applied to inhibit the ice formation in a water bath and to ensure the consistent flow of water mixture during the whole process.

During the experiment, the required pressure was maintained in the cell vessel and operating temperature in the temperature bath (having CO_2 with 99.99% purity). As the operating conditions related to pressure and volumes are achieved, cell valves were finally opened. Consequently, the experiment was held for 1200 min. After the completion of the experiment, hydrate decomposition was attained by reducing the given pressure to atmospheric pressure. The HPVA system was expelled with He gas to ready the apparatus for the next experiment and removed the sample cell from the system [5]. Then the obtained data of pressure- time (P-t) curve was analysed [23, 24].

3. Results and discussion

3.1. Effect of equilibrium moisture content

The amount of water contents in silica pores is vital for the formation of CO_2 hydrate in a batch fixed bed reactor (FBR). Thus; the calculated amount of water available for four prepared samples is first presented in **Table 2**. Initially, the results of equilibrium moisture content from each method are presented in which the confidence interval (CI) calculations were based on a 90% CI level. Previous studies used a magnetic stirrer and ultrasonic wave during sample preparation with the same intention to aid the dispersion of water inside silica pores [9, 25]. However, the sample prepared by method 4 with vigorous stirring using a high-speed blender in this work has the highest equilibrium moisture content with the lower CI which was 14.79 ± 0.34 wt%. As for methods 1-3 in this work, the amount of equilibrium moisture content was almost identical which was around 13.68 wt% but the CI for method 2 (gentle stirring by magnetic stirrer) was the lowest among those three with the value of ±0.51 wt%. Both methods 1 and 3 without stirring demonstrated quite high CI values, ± 2.45 and ± 2.87 wt% respectively as shown in **Fig. 2**. The relatively low CI obtained for methods 2 and 4 is explained by the need for stirring during sample preparation to ensure the water is well

distributed inside silica gel pores. These CI values also indicated that samples prepared from methods 2 and 4 had high reproducibility as compared to methods 1 and 3 as shown in **Fig. 2**.

3.1.1. Effect of pressure drop

Three sets of experiments were performed for each sample preparation method (methods 1-4) for assessing hydrate and their average experiment for P-t curve is discussed briefly. For the sake of maximum CO_2 uptake, an experimental duration of 1200 min was studied. Thus, the P-t curve for the best result attained in the IGCC conditions was preferred and presented in detail. **Fig. 3** (a-d) shows the analysis of P-t curves for all the four samples prepared during the present research. These curves were observed during the hydrate formation experiment, which shows about 2 bar pressure drop after 1200 min. It is due to the complete CO_2 dissolution in silica gel pores up to 33.5 bar. **Fig. 3** (d) shows the two-stage pressure drop trend and described the whole CO_2-water dissolution in water which was present in the pores of silica gel [20].

When the pressure dropped from 35 to 33.8 bar, it can be indicated by first-stage drop of pressure from point a-c. During the process, point a-b directs that CO_2 dissolved in water takes place in about 5 minutes. It has been stated that labile clusters formation takes place successfully upon dissolution of gas molecules in water. Concurrently, sharing forces start dominating to increase the disorders that show no pressure drop from point b-c. It has been stated that this point of primary nucleation is a continuous process during which the cluster size agglomeration approach critically at c point. It has been said that the time period from point a to c is known as induction time during hydrate formation stage [20].

Furthermore, it was observed that around 10 min is the fast induction time with the use of FBR and agreed well with already reported data [9, 11, 26, 27]. Secondly, after point c, the

next pressure drop stage was detected immediately and known as the hydrate growth at point d. Finally, two pressure drop stages were observed after 100 minutes (point d) before it became a plateau started approximately at 1000 minutes. For the highly stirred sample (method 4), a constant pressure stage was observed after 500 minutes, followed by method 3 (800 minutes), method 1 (900 minutes) and method 2 (1200 minutes).

3.1.2. CO_2 solubility in water

Since the experiments were conducted in batch mode or isochoric condition, the total number of moles of CO_2 consumed can easily be calculated by using the ideal gas law. The number of moles of CO_2 in H_2O was calculated to be 0.0438 where the value of Henry's constant at 275 K was obtained [12]. This value was not considered for the justification of hydrate formation because the value of Henry's constant in their work was calculated at atmospheric pressure that was not the same as the operating pressures employed in this work. However, this value was presented in **Fig. 4** (a) for comparison purposes. Thus, the equilibrium mole fraction of CO_2 in the water at various operating temperatures and pressures plotted by Servio and Englezos [24] can be used to compare the hydrate formation in the system.

Accordingly, temperature and pressure conditions (275.95 K and 20 bar) represents 0.017 value for equilibrium mole fraction in literature. In the present work, the hydrate formation was inveterate when the total experimental mole fraction was higher than the equilibrium mole fraction at the experimental conditions (275 K and 35 bar). Based on the given data the equilibrium mole fraction was found to be 0.016 at a specific temperature (275 K) and pressure (35 bar). **Fig. 4** (a) illustrates the total mole fraction of CO_2 consumed in H_2O for all four samples throughout the experiments. The red dashed line in **Fig. 4** (a) shows the total CO_2 dissolved in water at the experimental conditions in which further CO_2 is consumed after that is known as the growth of hydrate. In the case of method 4, the mole fraction of CO_2

consumption was 0.080 as compared to method 3, having 0.069 mole fraction of CO_2. Further, there were low mole fraction values of 0.072 and 0.0783 observed for method 1 and 2 respectively. While **Fig. 4**(b) illustrates the mole fraction of CO_2 consumed during hydrate growth. The highest total number of moles of CO_2 involved in hydrate formation was observed for the sample prepared by using method 4 and 2 is 0.06. While the total number of mole fractions for method 1 is 0.10 and 0.043 respectively as shown in **Fig. 4**(b).

3.2. Effect of vigorous stirring on CO_2 hydrate formation

3.2.1. Water to hydrate conversion and CO_2 uptake

Table 3 shows the summary of results obtained when the experiments were repeated three times for all four samples to analyse the reproducibility of the results. **Fig. 5**(a-b) illustrates the conversion of water into hydrate and carbon dioxide uptake for samples prepared by method 1 to 4. The CI for samples with a stirring process (method 2 and 4) was lower than samples without stirring (methods 1 and 3). Hence, the observed results explain the advantages of the vigorous stirring process during sample preparation as the water contents entered inside silica gel pores is overcome and beneficial for the utilisation of water in hydrate formation [27].

Total water to hydrate conversion and gas uptake showed the significance of vigorous stirring. The prepared sample during method 4 represents the highest conversion of water into hydrate with 40.5 ± 2.28 mol% value followed by method 2 (40.3 ± 3.42 mol%), method 1 (40.0 ± 4.84 mol%) and method 3 (37.9 ± 4.46 mol%). As the sample has a highest equilibrium moisture content, the highest water to hydrate conversion can be achieved due to vigorous stirring. Consequently, it was observed that the gas uptake has a direct relation to the quantity of water to hydrate conversion. Therefore, methods 1, 2 and 4 show CO_2 uptake of 3.9 mmol of CO_2 per g of H_2O, higher than method 3, having 3.7 mmol of carbon dioxide per gram of

water. However, method 4 consumed the highest molecules of CO_2 molecules which is 0.29 mmol followed by methods 2, 1 and 3 with values of 0.27, 0.26 and 0.26 mmol respectively.

Wherein the formation of methane hydrate for the sample (a mixture of silica and water) stirred at the 3700 rpm speed attained the highest gas uptake. Additionally, it has been mentioned that the gas to solid ratio in the gas hydrate is high as 1 ft^3 of hydrate contains 150–180 ft^3 of gas/ ft^3 of water [19]. Similarly, high regeneration and repeatability were better as compared to past studies using silica sand and pure water for CO_2 hydrate formation observed by Mekala et al. [28]. It represented the 0.06 moles of CO_2/ mole of H_2O as the highest uptake of CO_2 gas by 0.16 mm of silica sand. The reason behind the highest CO_2 uptake attained during the present study by method 4 is due to the 14.79% moisture content. Silica gel inhibits the coalescence of the droplets surrounds water droplets. Thus, increasing the amount of water inside silica pores. It has been mentioned that the high rate of mixing can be linked with low range particles which increased the gas-water interfacial surface area for hydrate formation due to the presence of dispersed water phase [29].

Moreover, it has been stated that a small angle of contact was associated with liquid range and a greater contact angle was affiliated with liquid beads (compact liquid droplets) exist on the surface. This contact angle is closely related to the spreadability or wettability. According to that, a small contact angle ($< 90^o$) increase the interaction between CO_2 gas-water with porous medium and as a result, enhancing hydrate formation [30]. It has been also added that small bubbles and droplets gives a minimum surface area due to their spherical nature for a fixed volume and increases the surface tension of water [31]. Thus, the use of vigorous stirring that dispersed water molecules is expected to reduce the surface tension of water inside silica pores and increases the rate of hydrate formation.

3.2.2. Rate of hydrate formation

Fig. 6 illustrates the rate of hydrate formation in 1200 min with the addition of the first 150 min. At 1200 min, the rate of hydrate formation could not be seen clearly, thus the comparison was done for the first 150 min. As method 4 uses vigorous stirring during its preparation, therefore, showed the fastest kinetics with the rate (0.05 mmol of carbon dioxide per gram of water per min) of hydrate generation and followed by methods 2, 1 and 3. The slowest initial rate can be demonstrated by method 3, which is almost 40% slower than method 4. The kinetics for all methods were almost the same after 120 minutes of the experiments. Thus, the hydrate formation rate for the samples prepared with stirring (methods 2 and 4) was better than the methods without stirring (methods 1 and 3). Overall, the sample prepared by method 4 showed the best results. On the other hand, the silica sand of 0.16 mm used by the previous study represents the 0.006 moles of CO_2/mol of H_2O/h as the rate of hydrate formation [28].

3.3. Comparison of experimental duration

In general, hydrate formation is known to be a slow process since it involves several stages namely dissociation, nucleation and hydrate growth stages. Normally, studies have been performed between 60 to 1200 minutes by previous researchers because hydrate growth started to slow down between these periods [28, 32]. The highest water conversion to hydrate reported by the literature and this work was around 60 mol%. Thus, some investigations in this work examined more than 1200 minutes to further explore the growth of hydrate. Experiments were performed by employing samples in a pure gas system at different driving forces and also one experiment in a fuel gas system. The results for consumed gas are reported and compared with the experiment performed at 1200 minutes.

3.3.1. CO_2 solubility in water

Fig. 7 (a-c) illustrates the solubility of CO_2 in water for several long experiments in pure CO_2 gas and fuel gas systems. In this investigation, the bed height of 3 cm was employed unless

otherwise stated. Generally, the trend of CO_2 solubility in water was increased for all experiments as time increased. Only experiments that employed zeolite 13X did not show any improvement after 1200 min. Additionally, X13-5 (13X contacted with 5.6 mol% THF + 0.01 mol% SDS) did not show any hydrate formation at all after 2500 min. However, the hydrate formation was observed for X13-5 with reduced bed height (3-2 cm) with no further hydrate growth observed after 400 min. Additionally, the most significant result was observed for T1-5 (having 5.6 mol% of THF and 0.01 mol% of SDS), at 2 cm bed height wherein the formation of hydrate occurred after 2500 min duration at 283 K and 58 bar in fuel gas mixture system. Moreover, the growth of hydrate was expected to continue because the specific number of moles of carbon dioxide dispersed in H_2O did not plateau within this period. However, for long experiments in batch FBR, the trend of solubility of CO_2 in water was not consistently increased due to a series of equilibrium states [33]. In conclusion, the dissolution of carbon dioxide in H_2O for both pure CO_2 and fuel gas systems for the long experiment was slightly improved by employing mesoporous silica gel.

For industrial-scale adaptation, key challenges include hydrate formation parameters such as operating temperature and pressure, reactor and process design to handle solid CO_2 hydrate formation inside the reactor, and continuous production of gas hydrate [34]. Wherein the idea is to improve water dispersion to enhance water/gas contact area, simultaneously enhance the kinetics of hydrate formation. Furthermore, a series of fixed bed reactors is necessary to provide a continuous multistage process in which the presence of promoters, porous medium, and process design optimization will improve separation efficiency where recycling will also become very important to reduce energy consumption and costs. This configuration will improvise the four steps' concept of the "Skarstrom cycle" which lead to four steps of

continuous hydrate formation namely hydrate formation, depressurization, hydrate decomposition and pressurization.

3.3.2 Water conversion to hydrate

Fig. 8 illustrates that as the duration of the experiment went on, the total water conversion to hydrate increased where only zeolite 13X did not show a significant increment. The maximum increment was observed for T1-5 in fuel gas mixture at 283 K and 58 bar with the increment of 13.82 mol% where hydrate growth could not be observed in the experiment that was only performed in 1200 minutes as shown in **Table 4**. This was followed by silica contacted with SDS (275 K and 36 bar) with the value of 58.63 mol% after 4000 min, the increment of 6.62 mol%. Moreover, the experiment by employing silica contacted with water also showed a comparable increment which was around 3.50 mol% at the temperatures of 275 and 280 K respectively. T1-5 also showed an increment in pure CO_2 and fuel gas mixture with 2 and 1.61 mol% respectively. In conclusion, the water conversion to hydrate was slightly improved as the duration of the experiment increased.

As for the fuel gas system, some researchers employed the FBR and STR [35, 36]. Park et al. [17] found that the phase equilibrium was shifted to the higher temperature region as the particle size of silica gel increased from 6 to 100 nm. However, they concluded that the hydrate phase equilibrium was shifted to the inhibition region of bulk water (STR) by using silica gel in FBR due to the presence of geometrical constraints (capillary effect). **Fig. 9** shows that the use of promoters in the STR such as 3 mol% TBAB [36] and 5.6 mol% THF [17] promoted the phase equilibrium to the IGCC conditions with the need for stirring during hydrate formation.

Zhang et al. [37] performed measurements of equilibrium level for the THF-SDS-CO_2-N_2-H_2O system at a fixed SDS concentration of 1000 ppm and various concentrations of THF in the presence of glass beads and the phase equilibrium shifted to a higher temperature (293 K at 90 bar) by increasing THF concentrations from 0–5 mol%. This indicated that the presence of THF can greatly increase the driving force of the system which also means mitigating the hydrate formation condition [20, 37].

Besides, Babu(b) et al. [32] investigated the formation of hydrate in the system of $TBANO_3$-CO_2-H_2-H_2O where $TBANO_3$ is also known as one type of semi-clathrate hydrate such as TBAB. They discovered that by introducing $TBANO_3$ in a fuel gas mixture system, the heat of dissociation increased significantly and also this semi-clathrate hydrate is said to be more stable than the hydrate formed from fuel gas mixture. Consequently, this will contribute towards the shifting of hydrate phase equilibrium to the high-temperature region wherein this effect is expected if $TBANO_3$ is substituted by TBAB in that system. Due to poor environmental conditions, [38, 39], there is a strong urge to advance sustainable resources [40, 41] and renewable technologies [42, 43] to condense the emission of CO_2 and control global warming [44]. Hence, combined promoters are outstanding substances that have excellent capture of CO_2 from different industrial plants.

Recently, Babu et al. [45] managed to observe CO_2 hydrate formation for 279-287 K and 40-60 bar by using 5.56 mol% of THF during batch STR. Then, Zheng et al. [11] managed to observe CO_2 hydrate formation at 60 bar and 285 K for 5.56 mol% of THF contacted with silica sand inside batch FBR which demonstrates the continued interest in improving hydrate formation with FBR to make it instantly feasible for the operating conditions of IGCC. Thus, the application of T1-5 (having 5.60 mol% of THF and 0.01 mol% of SDS) combined-

promoters in the FBR using in this work, thermodynamically shifted the hydrate phase equilibrium of fuel gas mixture to the IGCC conditions affiliated with silica gel was expected due to the thermodynamic effect of THF.

4. Conclusions

The HPVA was used to analyse the formation of the hydrate and to determine the experimental P-t curve for the CO_2 solubility in water via Henry's law. As method 4 utilize vigorous stirring during sample preparation, obtained the highest equilibrium moisture content (14.79 wt%). The repeatability of equilibrium moisture content and gas uptake attained for sample 4 was high as compared to other methods (1, 2 and 3) with the CIs of ± 0.34 wt% and ± 0.19 mmol of carbon dioxide per gram of water respectively. This is because of the specific concentration of water inside the silica gel, increased the spread-ability and directed towards the high water to hydrate conversion of about 40.5 ± 2.28 mol% in 1200 min. While using experimental time of 2600 min, the most significant results were observed for T1-5 (2 cm bed height) at 283 K and 58 bar where no formation of the hydrate was observed in the first 1200 min, however, 13.82 mol% of water conversion to hydrate was observed in 2600 min. The results compared with the literature demonstrated that 55% greater gas uptake obtained others at the IGCC conditions was expected due to the employment of macro-porous silica inside horizontal batch FBR in their work. Thus, a dual-batch horizontal FBRs configuration with the employment of macro-porous or mesoporous silica gel contacts with combined-promoters is being proposed which enables a continuous operation similar to how pressure swing adsorption would operate. In future, the CO_2 gas uptake towards a high rate of hydrate formation with macro-porous or mesoporous silica gel and modified sample preparation methods are suggested.

Acknowledgement

The authors are grateful for the financial supports from the Universiti Sains Islam Malaysia (USIM) and from the Ministry of Higher Education Malaysia (MoHE) to carry on this research.

References

1. Aminu, M.D., et al., A review of developments in carbon dioxide storage. Applied Energy, 2017. 208: p. 1389-1419.
2. Yan, Z., et al., Enhanced CO2 separation in membranes with anion-cation dual pathways. Journal of CO2 Utilization, 2020. 38: p. 355-365.
3. Zhang, Y., et al., Simulation of Particle Mixing and Separation in Multi-Component Fluidized Bed Using Eulerian-Eulerian Method: A Review. International Journal of Chemical Reactor Engineering, 2019. 17(11).
4. Antenucci, A. and G. Sansavini, Extensive CO2 recycling in power systems via Power-to-Gas and network storage. Renewable and Sustainable Energy Reviews, 2019. 100: p. 33-43.
5. Hassan, M.H.A., et al., Kinetic and thermodynamic evaluation of effective combined promoters for CO2 hydrate formation. Journal of Natural Gas Science and Engineering, 2020: p. 103313.
6. Zhu, L., et al., Tech-economic assessment of second-generation CCS: Chemical looping combustion. Energy, 2018. 144: p. 915-927.
7. Scholes, C.A., et al., Membrane gas separation—physical solvent absorption combined plant simulations for pre-combustion capture. Energy Procedia, 2013. 37: p. 1039-1049.
8. Al-Juboori, O., et al., The effect of variable operating parameters for hydrocarbon fuel formation from CO2 by molten salts electrolysis. Journal of CO2 Utilization, 2020. 40: p. 101193.
9. Babu, P., R. Kumar, and P. Linga, Pre-combustion capture of carbon dioxide in a fixed bed reactor using the clathrate hydrate process. Energy, 2013. 50: p. 364-373.
10. Zheng, J., P. Zhang, and P. Linga, Semiclathrate hydrate process for pre-combustion capture of CO2 at near ambient temperatures. Applied Energy, 2017. 194: p. 267-278.
11. Zheng, J., et al., Impact of fixed bed reactor orientation, liquid saturation, bed volume and temperature on the clathrate hydrate process for pre-combustion carbon capture. Journal of Natural Gas Science and Engineering, 2016. 35: p. 1499-1510.
12. Meshram, S.B., et al., Investigation on the effect of oxalic acid, succinic acid and aspartic acid on the gas hydrate formation kinetics. Chinese Journal of Chemical Engineering, 2019. 27(9): p. 2148-2156.
13. Kumar, A., et al., Influence of contact medium and surfactants on carbon dioxide clathrate hydrate kinetics. Fuel, 2013. 105: p. 664-671.
14. Davidson, R., Pre-combustion capture of CO2 in IGCC plants. IEA Clean Coa l Centre, 2011: p. 98.
15. Torré, J.-P., et al., CO2 enclathration in the presence of water-soluble hydrate promoters: hydrate phase equilibria and kinetic studies in quiescent conditions. Chemical engineering science, 2012. 82: p. 1-13.
16. Peirce, S., et al., Structure and activity of magnetic cross-linked enzyme aggregates of bovine carbonic anhydrase as promoters of enzymatic CO2 capture. Biochemical Engineering Journal, 2017. 127: p. 188-195.
17. Park, S., et al., Hydrate-based pre-combustion capture of carbon dioxide in the presence of a thermodynamic promoter and porous silica gels. International Journal of Greenhouse Gas Control, 2013. 14: p. 193-199.
18. Pivezhani, F., et al., Investigation of CO2 hydrate formation conditions for determining the optimum CO2 storage rate and energy: Modeling and experimental study. Energy, 2016. 113: p. 215-226.

19. Dawson, R., et al., 'Dry bases': carbon dioxide capture using alkaline dry water. Energy & Environmental Science, 2014. 7(5): p. 1786-1791.
20. Tang, J., et al., Study on the influence of SDS and THF on hydrate-based gas separation performance. Chemical Engineering Research and Design, 2013. 91(9): p. 1777-1782.
21. Yang, M., et al., Effects of an additive mixture (THF+ TBAB) on CO2 hydrate phase equilibrium. Fluid phase equilibria, 2015. 401: p. 27-33.
22. Li, X.-S., et al., Hydrate-based pre-combustion carbon dioxide capture process in the system with tetra-n-butyl ammonium bromide solution in the presence of cyclopentane. Energy, 2011. 36(3): p. 1394-1403.
23. Diamond, L.W. and N.N. Akinfiev, Solubility of CO2 in water from− 1.5 to 100 C and from 0.1 to 100 MPa: evaluation of literature data and thermodynamic modelling. Fluid phase equilibria, 2003. 208(1-2): p. 265-290.
24. Servio, P. and P. Englezos, Effect of temperature and pressure on the solubility of carbon dioxide in water in the presence of gas hydrate. Fluid phase equilibria, 2001. 190(1-2): p. 127-134.
25. Park, S., et al., Hydrazine-reduction of graphite-and graphene oxide. Carbon, 2011. 49(9): p. 3019-3023.
26. Linga, P., R. Kumar, and P. Englezos, Gas hydrate formation from hydrogen/carbon dioxide and nitrogen/carbon dioxide gas mixtures. Chemical engineering science, 2007. 62(16): p. 4268-4276.
27. Babu, P., et al., A review of the hydrate based gas separation (HBGS) process for carbon dioxide pre-combustion capture. Energy, 2015. 85: p. 261-279.
28. Mekala, P., et al., Effect of silica sand size on the formation kinetics of CO2 hydrate in porous media in the presence of pure water and seawater relevant for CO2 sequestration. Journal of Petroleum Science and Engineering, 2014. 122: p. 1-9.
29. Wang, W., et al., Methane storage in dry water gas hydrates. Journal of the American Chemical Society, 2008. 130(35): p. 11608-11609.
30. Yuan, Y. and T.R. Lee, Contact angle and wetting properties, in Surface science techniques. 2013, Springer. p. 3-34.
31. Zisman, W.A., Relation of the equilibrium contact angle to liquid and solid constitution. 1964, ACS Publications.
32. Babu, P., et al., Thermodynamic and kinetic verification of tetra-n-butyl ammonium nitrate (TBANO3) as a promoter for the clathrate process applicable to precombustion carbon dioxide capture. Environmental science & technology, 2014. 48(6): p. 3550-3558.
33. Kobayashi, T. and Y.H. Mori, Thermodynamic simulations of hydrate formation from gas mixtures in batch operations. Energy conversion and management, 2007. 48(1): p. 242-250.
34. Pandey, J.S., et al., Enhanced Hydrate-Based Geological CO2 Capture and Sequestration as a Mitigation Strategy to Address Climate Change. Energies, 2020. 13(21): p. 5661.
35. Kumar, R., H.-j. Wu, and P. Englezos, Incipient hydrate phase equilibrium for gas mixtures containing hydrogen, carbon dioxide and propane. Fluid phase equilibria, 2006. 244(2): p. 167-171.
36. Kim, S.M., et al., Gas hydrate formation method to capture the carbon dioxide for pre-combustion process in IGCC plant. International journal of hydrogen energy, 2011. 36(1): p. 1115-1121.

37. Zhang, Y., et al., Hydrate phase equilibrium measurements for (THF+ SDS+ CO2+ N2) aqueous solution systems in porous media. Fluid Phase Equilibria, 2014. 370: p. 12-18.
38. Sehar, S., et al., Thermodynamic and kinetic study of synthesised graphene oxide-CuO nanocomposites: A way forward to fuel additive and photocatalytic potentials. Journal of Molecular Liquids, 2020: p. 113494.
39. Zhang, Y., et al., Effect of slot wall jet on combustion process in a 660 MW opposed wall fired pulverized coal boiler. 2019. 17(4).
40. Sher, F., et al., Development of biomass derived highly porous fast adsorbents for post-combustion CO2 capture. 2020. 282: p. 118506.
41. Rashid, T., et al., Formulation of Zeolite-supported Nano-metallic Catalyst and its Application in Textile Effluent Treatment. Journal of Environmental Chemical Engineering, 2020: p. 104023.
42. Al-Shara, N.K., et al., Design and optimization of electrochemical cell potential for hydrogen gas production. Journal of Energy Chemistry, 2021. 52: p. 421-427.
43. Razzaq, L., et al., Modeling Viscosity and Density of Ethanol-Diesel-Biodiesel Ternary Blends for Sustainable Environment. Sustainability, 2020. 12(12): p. 5186.
44. Sher, F., et al., Enhancing hydrogen production from steam electrolysis in molten hydroxides via selection of non-precious metal electrodes. 2020. 45(53): p. 28260-28271.
45. Babu, P., H.W.N. Ong, and P. Linga, A systematic kinetic study to evaluate the effect of tetrahydrofuran on the clathrate process for pre-combustion capture of carbon dioxide. Energy, 2016. 94: p. 431-442.

List of Tables

Table 1. The relative concentration of promoter, SiG (silica gel) and water used during samples preparation.

Promoter Type	Concentration (mol %)	Mass of promoter (g)	Mass of dry SiG (g)	Mass of water (g)
THF	3.00	5.23	2.50	42.27
SDS	0.01	0.08	2.50	47.42

583 **Table 2.** Summary of equilibrium moisture content in wet SiG (silica gel) for samples
584 prepared by method 1-4.

Sample	Experiment	SiG (wet) (g)	SiG (dry) (g)	Equilibrium moisture content (wt%)	Mean Equilibrium moisture content (wt%)	SD	90% C1 (±)
Method 1	1	0.06	0.05	15.05	13.56	2.11	2.45
	2	0.08	0.07	12.07			
Method 2	1	0.06	0.05	13.33	13.64	0.44	0.51
	2	0.09	0.07	13.95			
Method 3	1	0.05	0.04	16.52	13.83	2.47	2.87
	2	0.11	0.10	11.65			
Method 4	1	0.14	0.12	15.00	14.79	0.29	0.34
	2	0.10	0.08	14.58			

585

586

Table 3. Specifications of highest water conversion, CO_2 uptake and CO_2 hydrate formation at 275 K and 35 bar in 1200 minutes.

Sample	**Experiment**	**Water conversion to hydrate**	**Mean water conversion to hydrate**	**SD**	**CO_2 uptake**	**Mean CO_2 uptake**	**SD**	**CO_2 formed in hydrate**	**Mean CO_2 produced during hydrate**
		(mol%)	(mol%) (90% CI)		(mmol of CO_2/g of H_2O)	(mmol of CO_2/g of H_2O) (90% CI)		(mmol)	(mmol)
Method 1	1	37.8	40.0± 4.84	5.1	3.7	3.9± 0.47	0.5	0.24	0.26
	2	36.4			3.5			0.23	
	3	45.9			4.4			0.30	
Method 2	1	36.8	40.3± 3.42	3.6	3.6	3.9 ±0.38	0.4	0.24	0.27
	2	40.1			3.9			0.27	
	3	44.0			4.3			0.29	
Method 3	1	34.8	37.9± 4.46	4.7	3.4	3.7±0.47	0.5	0.24	0.26
	2	43.3			4.2			0.29	
	3	35.6			3.4			0.24	
Method 4	1	40.6	40.5± 2.28	2.4	3.9	3.9±0.19	0.2	0.29	0.29
	2	38.0			3.7			0.28	
	3	42.8			4.1			0.31	

Table 4. Evaluation of water to hydrate conversion for long and short experiments at various experimental conditions.

Sample	Gas system	Experiment conditions	Experiment duration (min)	Water conversion to hydrate (mol%)	Increment (mol%)
SiG-SDS	Pure CO_2	275 K, 36 bar	4000	58.63	6.62
			1200	52.01	
SiG-H_2O	Pure CO_2	275 K, 36 bar	2500	44.10	3.47
			1200	40.63	
T1-5	Pure CO_2	275 K, 30 bar	2600	26.26	2.00
			1200	24.26	
SiG-H_2O	Pure CO_2	280 K, 36 bar	5000	9.73	3.72
			600	6.01	
X13-5, 2 cm	Pure CO_2	275 K, 36 bar	2600	6.25	0.43
			1200	5.82	
T1-5, 2 cm	Fuel gas mixture	283 K, 58 bar	2600	13.82	13.82
			1200	0.00	

List of Figures

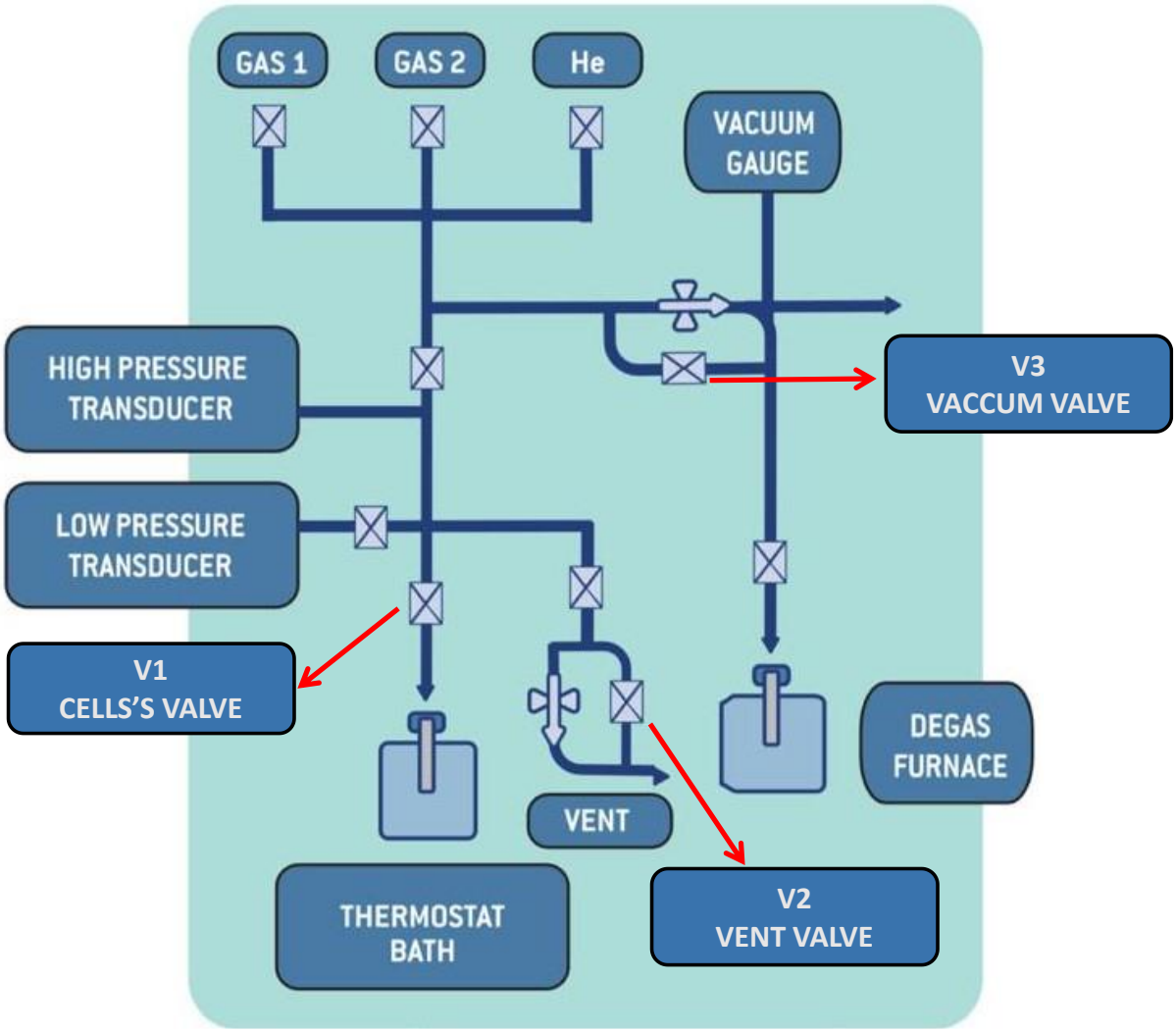

Fig. 1 . High pressure volumetric analyser (HPVA).

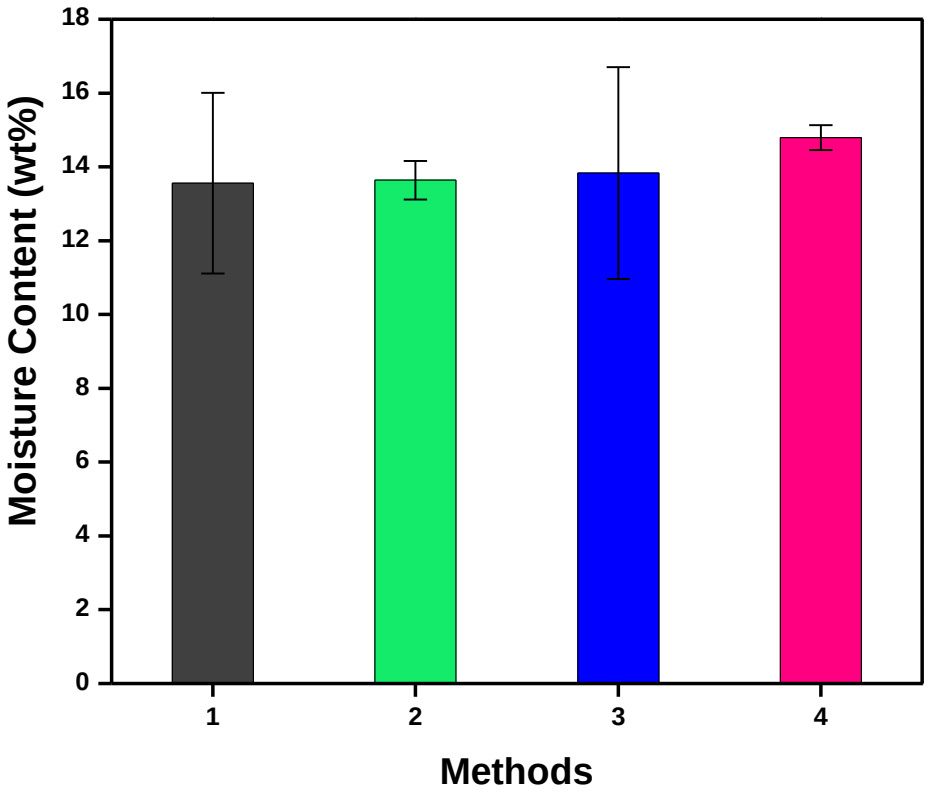

Fig. 2. The equilibrium moisture content in wet silica gel for samples prepared by methods 1-4.

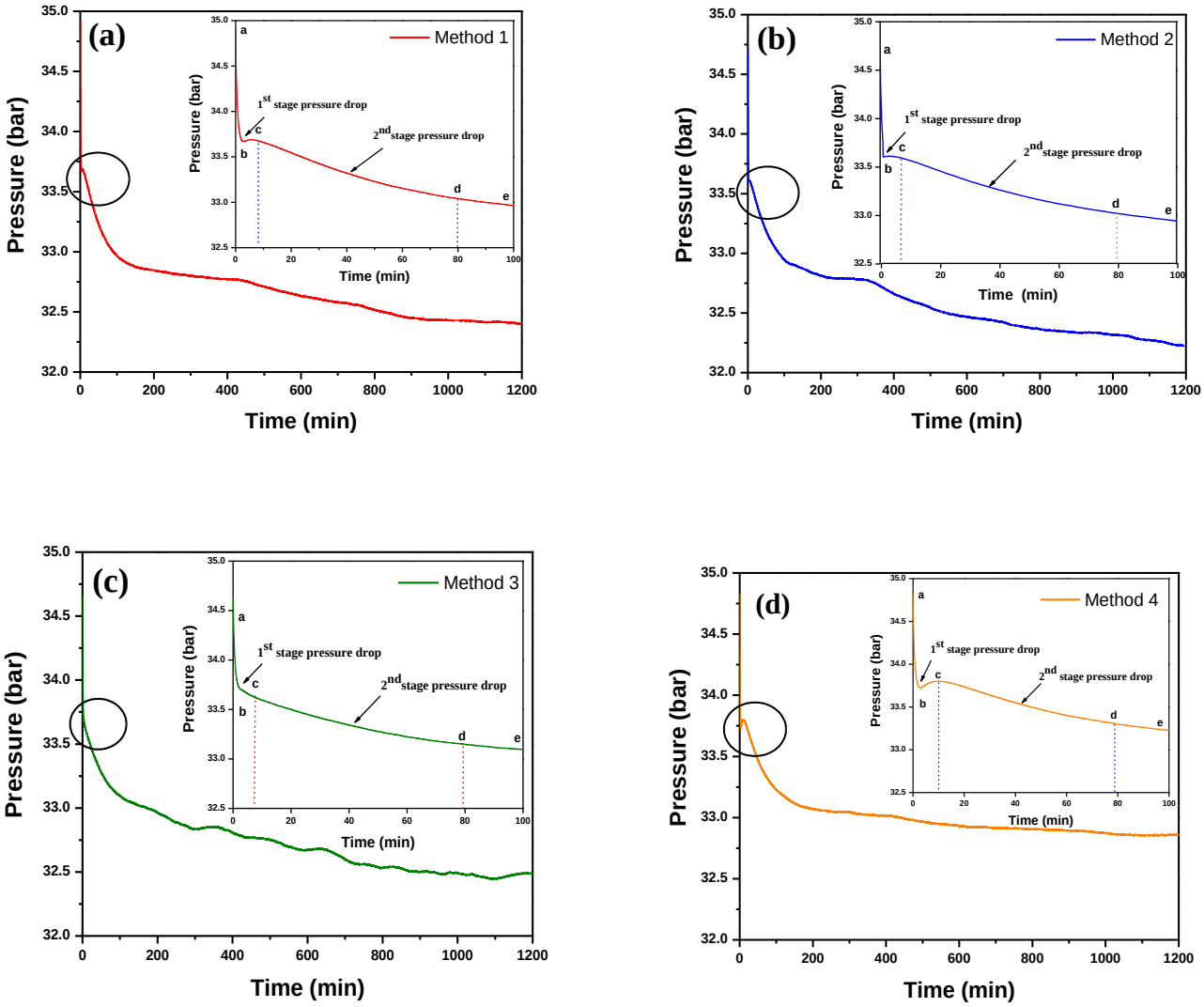

Fig. 3. Representation of P-t curves for two-stage pressure drop in first 100 and 1200 min for different methods; (a) Method 1, (b) Method 2, (c) Method 3 and (d) Method 4.

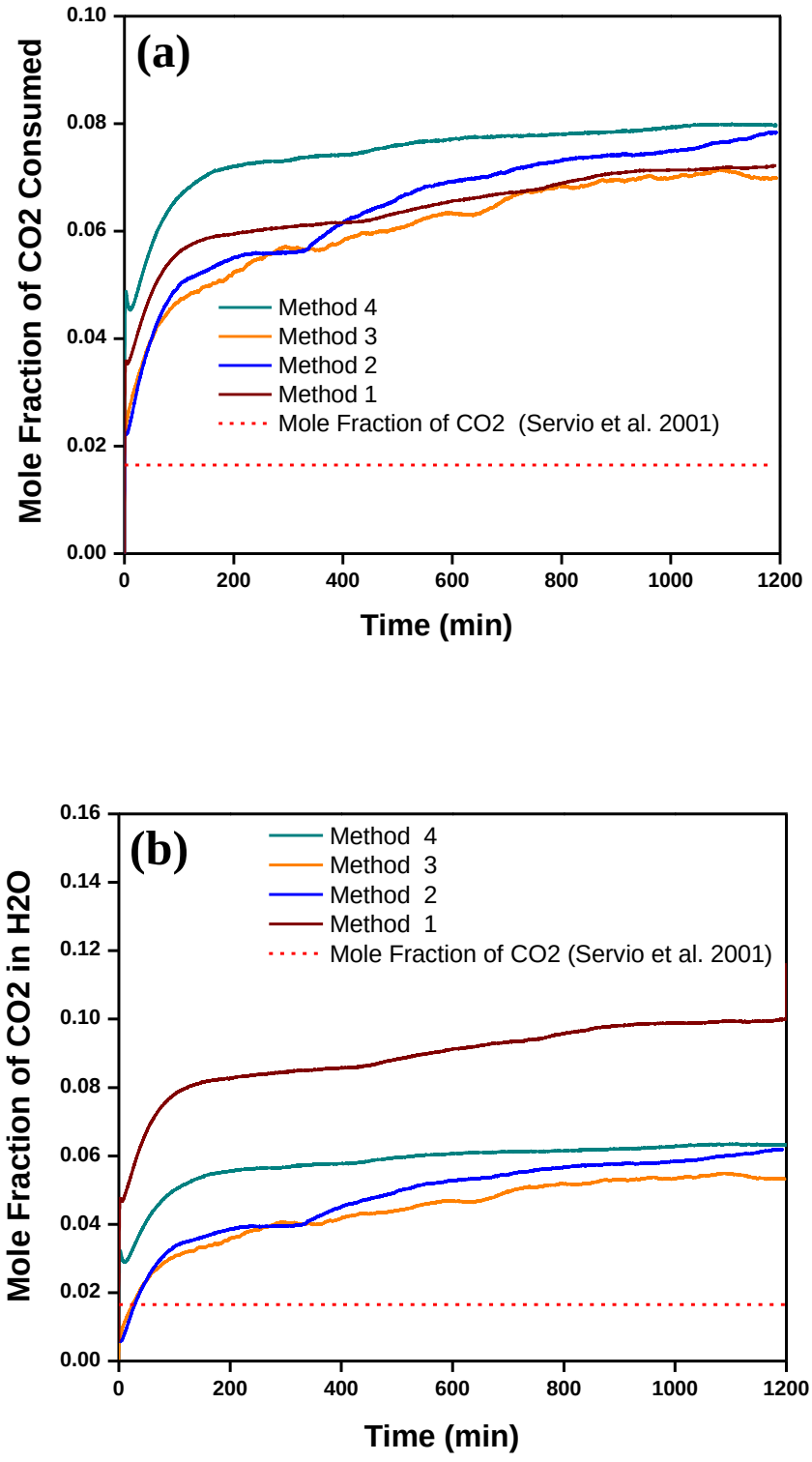

Fig. 4. Mole fraction of CO_2 in wet silica gel for methods 1– 4 at 275 K and 35 bar in 1200 min; (a) Total mole fraction of CO_2 and (b) Mole fraction of CO_2 during hydrate growth.

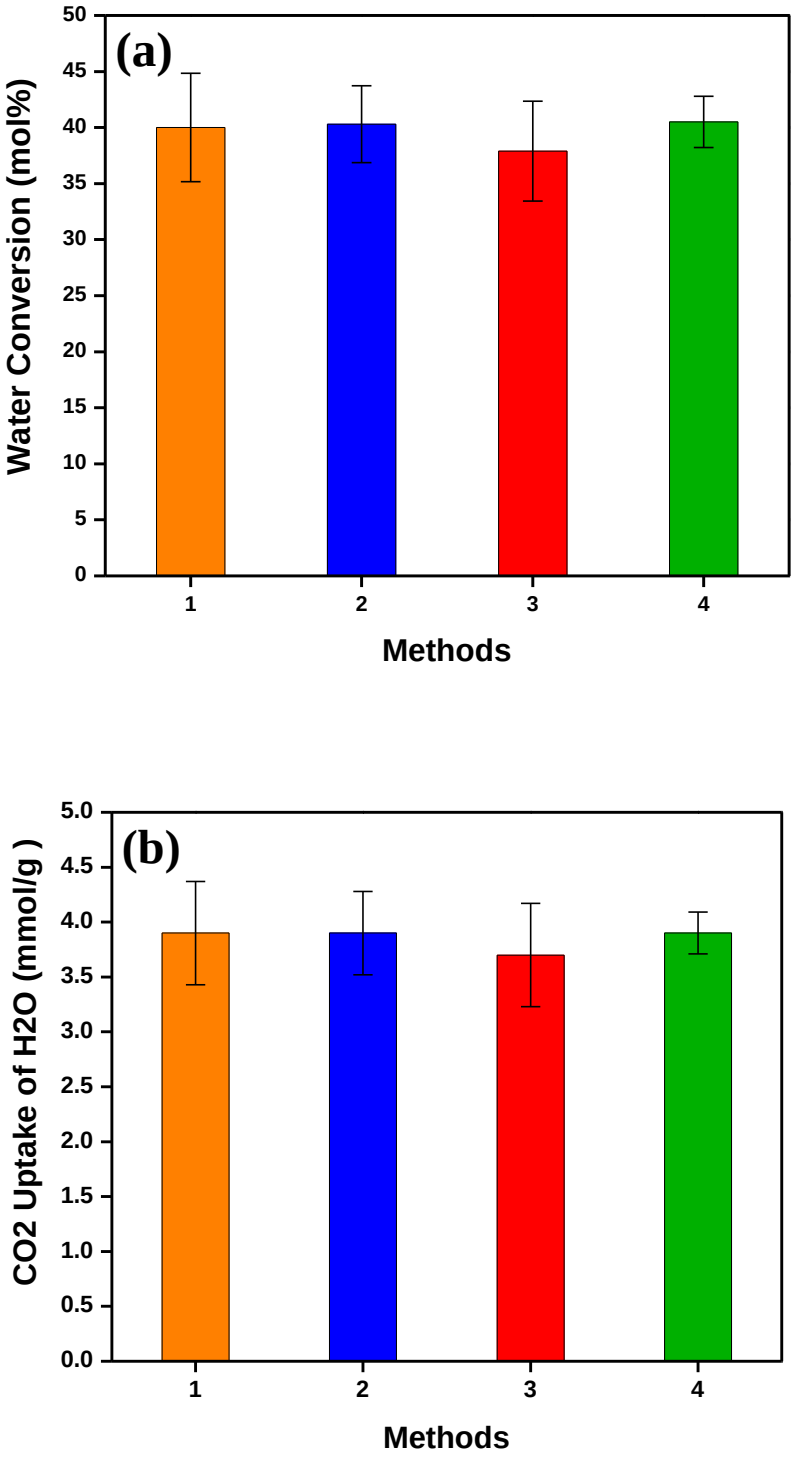

Fig. 5. Comparison of methods 1 to 4 at 275 K and 35 bar for 1200 minutes; (a) H_2O to hydrate conversion and (b) CO_2 update of H_2O.

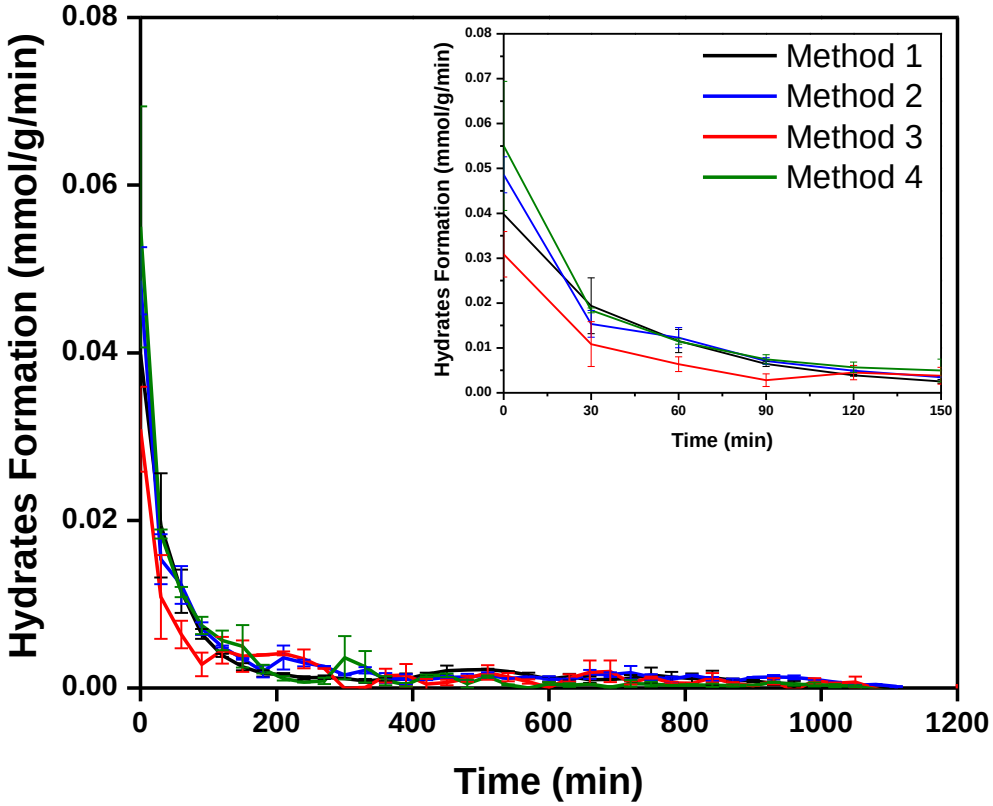

Fig. 6. Hydrate formation for 1200 min and first 150 min for methods 1to 4.

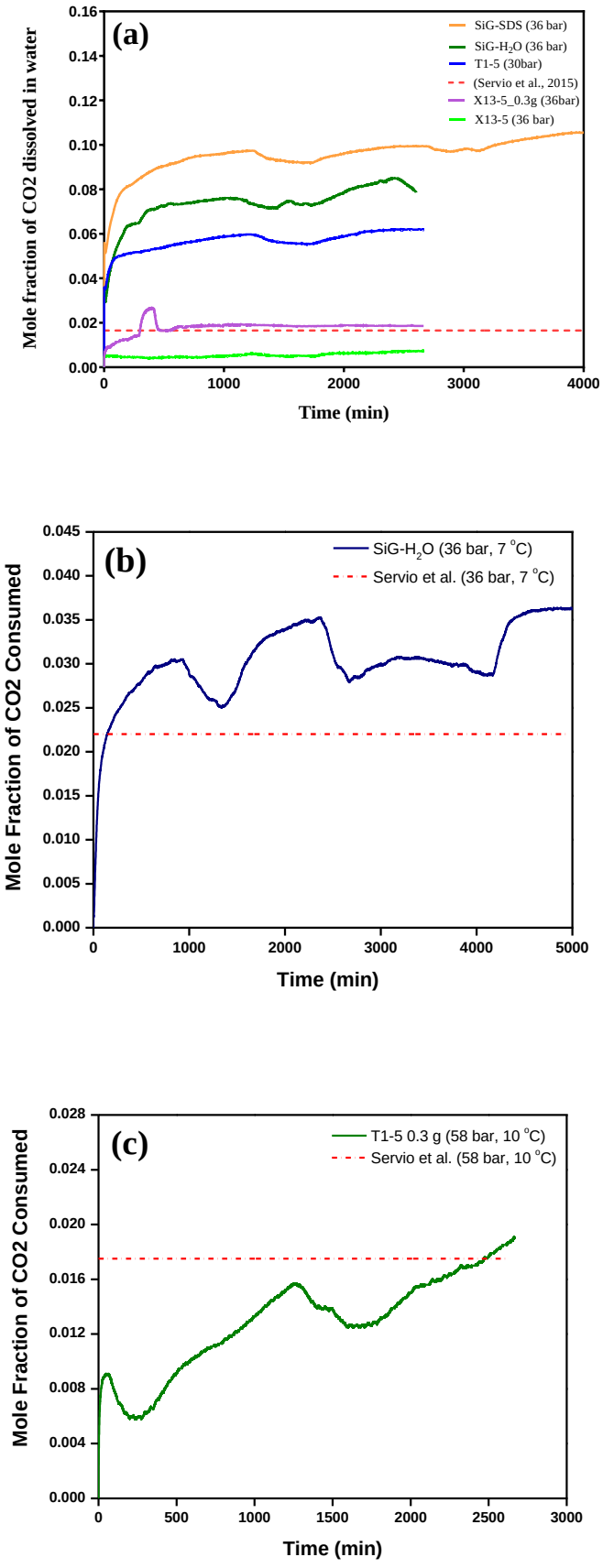

Fig. 7. CO_2 solubility in water for long experiments; (a) Pure CO_2 gas system at 275 K and various driving forces, (b) Pure CO_2 gas system at 280 K and 36 bar and (c) Fuel gas system at 283 K and 58 bar.

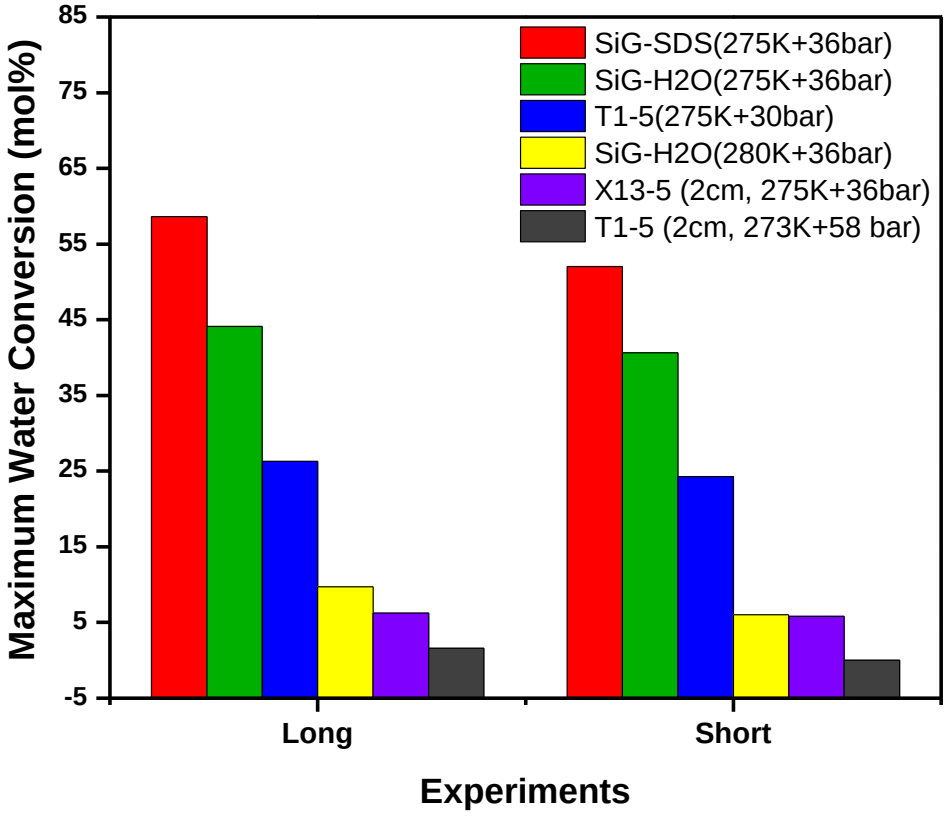

Fig. 8. Comparative evaluation of exchange of water to hydrate at long and short experimentation time.

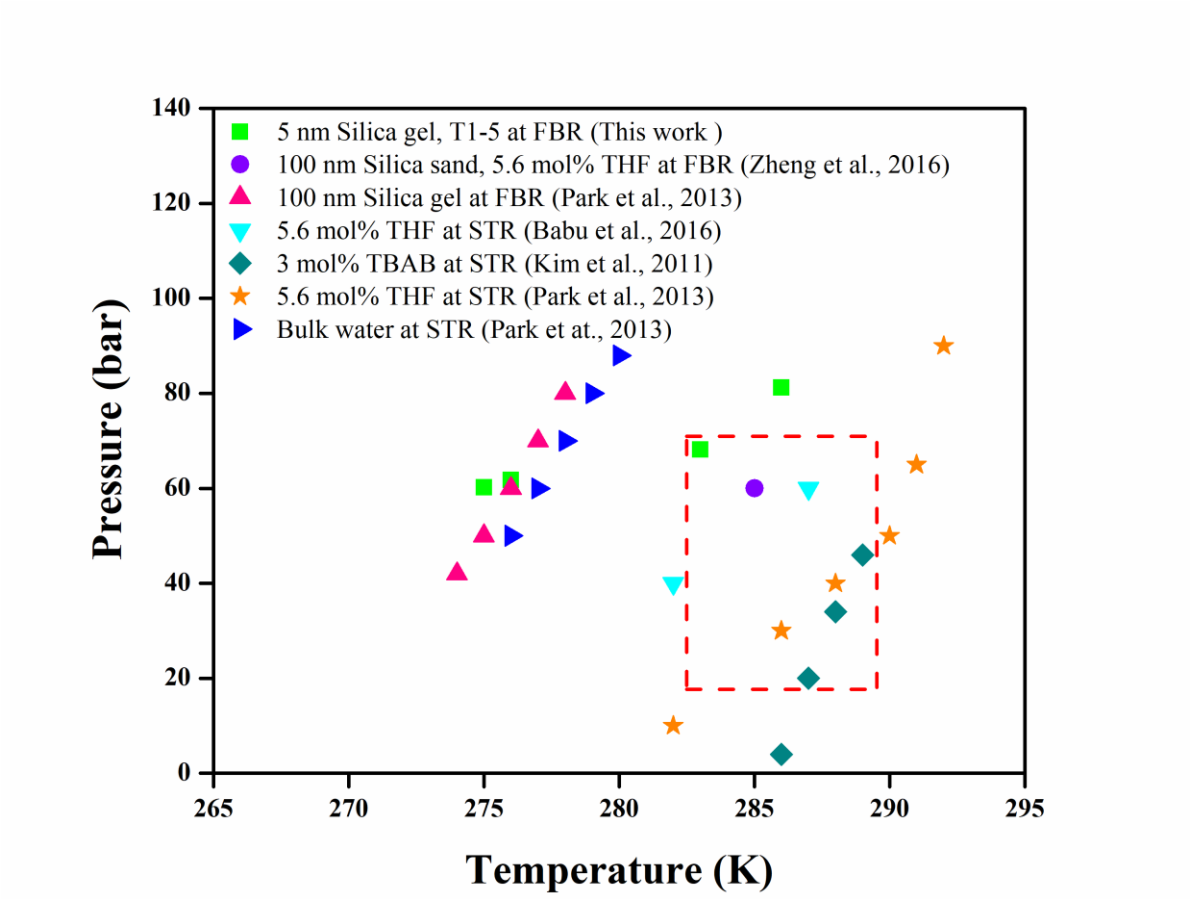

Fig. 9. Comparison of equilibrium based hydrate formation for fuel gas with IGCC operating conditions of the present study with Zheng et al. [11], Park et al. [17], Babu et al., [45] and Kim at al. [36].